Redox Biology 83 (2025) 103633

Contents lists available at ScienceDirect

Redox Biology

journal homepage: www.elsevier.com/locate/redox

Cytoglobin scavenges intracellular hydrogen peroxide and regulates redox signals in the vasculature

Frances Jourd'heuil [a], Clinton Mathai [a], Le Gia Cat Pham [a], Kurrim Gilliard [a], Joseph Balnis [a,b], Katherine A. Overmyer [c,d], Joshua J. Coon [c,d,e], Ariel Jaitovich [a,b], Benoit Boivin [f], David Jourd'heuil [a,*]

[a] Department of Molecular and Cellular Physiology, Albany Medical College, Albany, NY, USA
[b] Division of Pulmonary and Critical Care Medicine, Albany Medical College, Albany, NY, USA
[c] Department of Biomolecular Chemistry, University of Wisconsin-Madison, Madison, WI, USA
[d] Morgridge Institute for Research, Madison, WI, USA
[e] Department of Chemistry, University of Wisconsin-Madison, Madison, WI, USA
[f] Department of Nanoscale Science & Engineering, University at Albany, Albany, NY, USA

ARTICLE INFO

Keywords:
Cytoglobin
Glycolysis
Hydrogen peroxide
Reactive oxygen species
Hemoglobin
Peroxidase
Peroxiredoxin
Smooth muscle
Fibroblast
Carotid artery
Redox signal

ABSTRACT

The oxidant hydrogen peroxide (H_2O_2) serves as a signaling molecule that alters many aspects of cardiovascular functions and contributes to cardiovascular diseases. Recent studies suggest that cytoglobin – a member of the globin family - may promote electron transfer reactions with proposed functions in H_2O_2 decomposition. In the present study, we directly examined the ability of cytoglobin to decompose H_2O_2. Carotid arteries from cytoglobin knockout mice were more sensitive to glycolytic inhibition by H_2O_2 than arteries from wild type mice. In addition, the ectopic expression of cytoglobin in cultured cells limited the inhibitory effect of H_2O_2 on glycolysis and reversed the oxidative inactivation of the glycolytic enzyme GAPDH. Cytoglobin facilitated the reduction of the thiol-based H_2O_2 sensor Hyper7 after H_2O_2 challenge. The specific substitution of one of two cysteine residues on cytoglobin (C83) inhibited its antioxidant activity, as did the substitutions at the proximal and distal histidine residues. *In vitro*, direct measurements of H_2O_2 concentrations indicated that purified cytoglobin consumes H_2O_2 at rates comparable to that of peroxiredoxin 2 and that it competitively inhibits the hyperoxidation of peroxiredoxin 2. We propose that cytoglobin may serve as a regulator of intracellular redox signals initiated by H_2O_2.

1. Introduction

Although reactive oxygen species (ROS) have been implicated in the etiology of cardiovascular disease (CVD) [1], their specific roles in promoting pathological hallmarks such as vascular remodeling and atherosclerosis are still unclear. For example, whether overproduction of ROS simply contributes to undifferentiated oxidative injury or more specifically dysregulates redox signals that are important for disease progression is still open for discussion. Clearly, significant progress has been made over the past two decades in the characterization of oxidant producing enzymes and the antioxidant systems that might provide counter-regulation. Redox signaling that requires 2 electron oxidation reactions often involve hydrogen peroxide (H_2O_2) as the chemical signal. Thus, an increasing list of oxidative post-translational modifications sensitive to H_2O_2 have been identified and shown to regulate key aspects of vascular physiology and pathophysiology. This includes regulation of blood pressure, hypertension, and vascular remodeling [2–6]. The exact mechanism by which H_2O_2 and other ROS might propagate redox signals is only beginning to be deciphered. In some cases, this might require reversible inhibition of antioxidant systems to allow for diffusion and reaction of the oxidant with its target [7,8]. Alternatively, conversion of H_2O_2 to organic hydroperoxides may be required to escape reductive inactivation [9]. New concepts have also emerged that paradoxically implicate antioxidant systems such as the peroxiredoxins in propagating redox signals [10,11]. Finally, some protein targets might be able to directly react with H_2O_2 and serve as redox sensors [12,13].

Past studies suggest that cytoglobin (CYGB) may be uniquely

* Corresponding author.
E-mail address: jourdhd@amc.edu (D. Jourd'heuil).

https://doi.org/10.1016/j.redox.2025.103633
Received 21 February 2025; Received in revised form 1 April 2025; Accepted 8 April 2025
Available online 12 April 2025

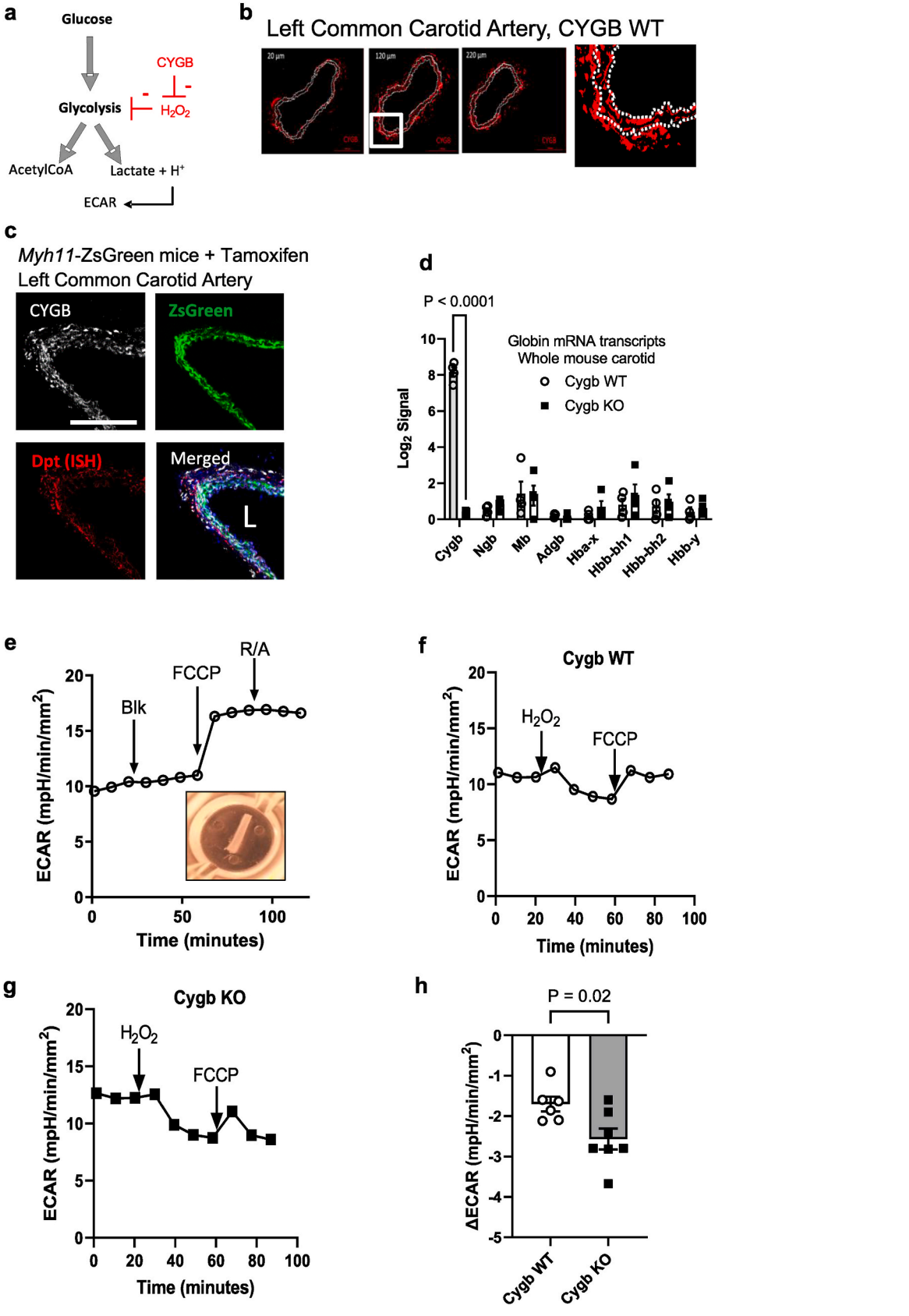

(caption on next page)

Fig. 1. Loss of cytoglobin increases the sensitivity of glycolysis to hydrogen peroxide in isolated mouse carotidarteries. a, Schematic of the proposed effect of hydrogen peroxide and cytoglobin on the glycolytic pathway. See Text for details. **b**, Representative indirect immunofluorescence staining for cytoglobin (red) in serial sections - 20, 120, and 220 μm from the bifurcation between the internal and external carotid artery - obtained from the left common artery of wildtype mice; scale bar is 200 μm; inset shows enlargement of the middle picture with cytoglobin staining in both the adventitia and media; white dotted line delineate the limit of the media, based on laminas autofluorescence. **c**, Representative indirect immunofluorescence staining for cytoglobin (CYGB), ZsGreen positive cells, and in situ hybridization (ISH) for dermatopontin (Dpt) mRNA in mouse carotid artery from tamoxifen-induced Myh11 ER^{T2} cre ZsGreen mice. Scale bar is 200 μm; L = lumen. **d**, Bulk RNA seq analysis was performed on the left common carotid artery of cytoglobin wildtype (Cygb WT) and knockout (Cygb KO) mouse littermates and results were queried for globin mRNA and plotted as the Log_2 signal for each transcript. Statistical analysis was performed using two-way ANOVA with Tukey's multi-comparisons test. **e**, Representative tracing of extracellular acidification rate (ECAR) measurements obtained from the carotid artery of WT mice. Arrows indicate sequential addition of PBS (Blk), FCCP, and rotenone with antimycin A (R/A). Insert, representative image of an isolated length of the mouse carotid artery prepared for metabolic flux analysis. **f** and **g**, Extracellular acidification profiles obtained from carotid arteries from cytoglobin wildtype (Cygb WT, f) and knockout (Cygb KO, g) mouse littermates. Arrows indicate the sequential addition of hydrogen peroxide (H_2O_2, 200 μM) and FCCP. **h**, Quantitation of the change in ECAR (ΔECAR) following the addition of hydrogen peroxide on carotid arteries obtained from cytoglobin wildtype (Cygb WT) and knockout (Cygb KO) mice. The time points used to calculate ΔECAR were the first and third points after addition of hydrogen peroxide. Each data point indicates one mouse. Statistical analysis was performed using unpaired Student's t-test.

positioned to support the handling of ROS in the vasculature. It is expressed in vascular smooth muscle cells [14–16] and its reaction with nitric oxide (NO), nitrite (NO_2^-), superoxide (O_2^-), and H_2O_2 have all been proposed to underpin its function in regulating vascular tone and injury [15–18]. Although the role of cytoglobin as an NO dioxygenase is relatively well established, the exact mechanism by which it may regulate H_2O_2 is less clear. One reason is that the second order rate constant for the reaction of H_2O_2 with cytoglobin is several orders of magnitude slower than known heme and thiol-based peroxidases such as catalase and peroxiredoxins [19]. This would preclude a direct role for cytoglobin as a physiologically relevant scavenger or target of H_2O_2, unless alternative mechanisms exist. There is little doubt that the deletion of cytoglobin in mouse models is associated with increased oxidant burden but these effects might be secondary and related, for example, to a dysregulated inflammatory response [20]. Alternatively, cytoglobin loss has been associated with changes in gene expression both *in vivo* and in cell cultures with apparent preferential changes in genes related to antioxidant systems [21–23], which might also explain the increase in resistance to H_2O_2.

In a recent study, we showed that vascular smooth muscle cytoglobin relocates from the cytosol to the nucleus in response to serum stimulation [16]. Once in the nucleus, cytoglobin may regulate gene transcription and DNA damage response pathways through interaction with the chromatin remodeler HMGB2 [16]. Significantly, we also established that the serum-dependent nuclear accumulation of cytoglobin required the H_2O_2 producing enzyme NOX4. This could be recapitulated in the absence of serum through treatment with H_2O_2. This led us to propose an alternative function for cytoglobin as a H_2O_2 sensor. In the present study, we establish that cytoglobin can directly remove H_2O_2 inside cells. We show that cytoglobin reverses the inhibitory effect of H_2O_2 on the glycolytic pathway. *In vitro*, we show that the reaction of H_2O_2 with cytoglobin is rapid enough to compete with the hyperoxidation of peroxiredoxin 2. Our results are consistent with a role for cytoglobin as a physiological target of H_2O_2.

2. Results

2.1. Loss of cytoglobin increases the sensitivity of the glycolytic pathway to H_2O_2 in mouse vessels

Past studies have shown that several glycolytic enzymes are highly sensitive to H_2O_2 mediated inhibition [12,13,24–26] and we reasoned that examination of glycolytic activity may serve as a surrogate to test for H_2O_2 sensitivity in isolated vessels and cells. In vessels, glycolysis provides a significant fraction of the basal bioenergetic requirement, even under fully aerobic conditions and in the absence of force generation [27]. Thus, in the first set of experiments, we determined whether cytoglobin deletion increased the sensitivity of isolated mouse carotid arteries to the H_2O_2-mediated inhibition of glycolysis (Fig. 1a). Indirect immunostaining of cytoglobin protein in wild-type mice confirmed the expression of cytoglobin in the media consistent with SMC association. However, we also found significant staining in the adventitia (Fig. 1b). To unequivocally establish the expression of cytoglobin in SMCs, we isolated carotid arteries from transgenic mice that express a tamoxifen-inducible Cre-recombinase driven by the SMC-specific *Myh11* promoter combined with a Cre-responsive zsGreen inserted at the *ROSA26* locus. Using this system, SMCs are permanently labeled with zsGreen once the mice are administered tamoxifen. We stained carotid artery cross sections for cytoglobin by indirect immunofluorescence and showed that cytoglobin immunostaining co-associated with ZsGreen positive medial cells (Fig. 1c). The expression of cytoglobin in cells populating the adventitia was also explored through co-immunofluorescence staining for dermatopontin (*Dpt*) mRNA, a fibroblast marker [28]. As shown in Fig. 1c, there was also significant co-association of *Dpt* with CYGB in the adventitia suggesting widespread expression of cytoglobin in adventitial fibroblasts in the mouse carotid.

Next, cytoglobin wild-type and knockout mice littermates (Cygb WT and Cygb KO mice) were generated as previously described [15]. Cytoglobin loss was verified by Western blot and indirect immunofluorescence analysis (Supplementary Figs. 1a and b). We performed a differential gene expression analysis on a bulk RNA seq from isolated left common carotid arteries. We queried this data set for the expression of globins (Fig. 1d) and established that cytoglobin mRNA exceeded the expression of any other globin transcripts by more than 10-fold. Deletion of cytoglobin did not alter the expression of the other globin transcripts (Fig. 1d).

Finally, glycolytic rates in vessels were assessed by measuring extracellular acidification rates (ECAR) using Seahorse XF technology. We isolated 2-mm length carotid artery segments and measured basal ECAR following the sequential addition of a blank, the mitochondrial uncoupler carbonyl cyanide *p*-trifluoromethoxyphenylhydrazone (FCCP) and a combination of two respiratory chain inhibitors rotenone and antimycin A (Fig. 1e). Addition of FCCP in the presence of glucose increased ECAR suggesting that the basal glycolytic rate of these vessels is limited by a low resting demand that can be increased through mitochondrial uncoupling with FCCP. The lack of effect of rotenone and antimycin A on ECAR indicated the absence of contribution from oxidative phosphorylation. There was also no difference in basal ECAR or FCCP-stimulated ECAR between wild-type and knockout mice (Supplementary Fig. 2). Treatment of the vessels with H_2O_2 resulted in a decrease in ECAR (Fig. 1f). However, the extent of the decrease in ECAR was significantly greater in cytoglobin knockout vessels compared to wildtype (Fig. 1f, g, and h). We also noted a collapse in FCCP-stimulated ECAR (Fig. 1f and g) and the vessels with cytoglobin deletion were unable to sustain a measurable increase, past a few minutes (Fig. 1g). Altogether, these results indicated a protective effect of cytoglobin against H_2O_2-mediated inhibition of glycolysis in mouse carotid arteries.

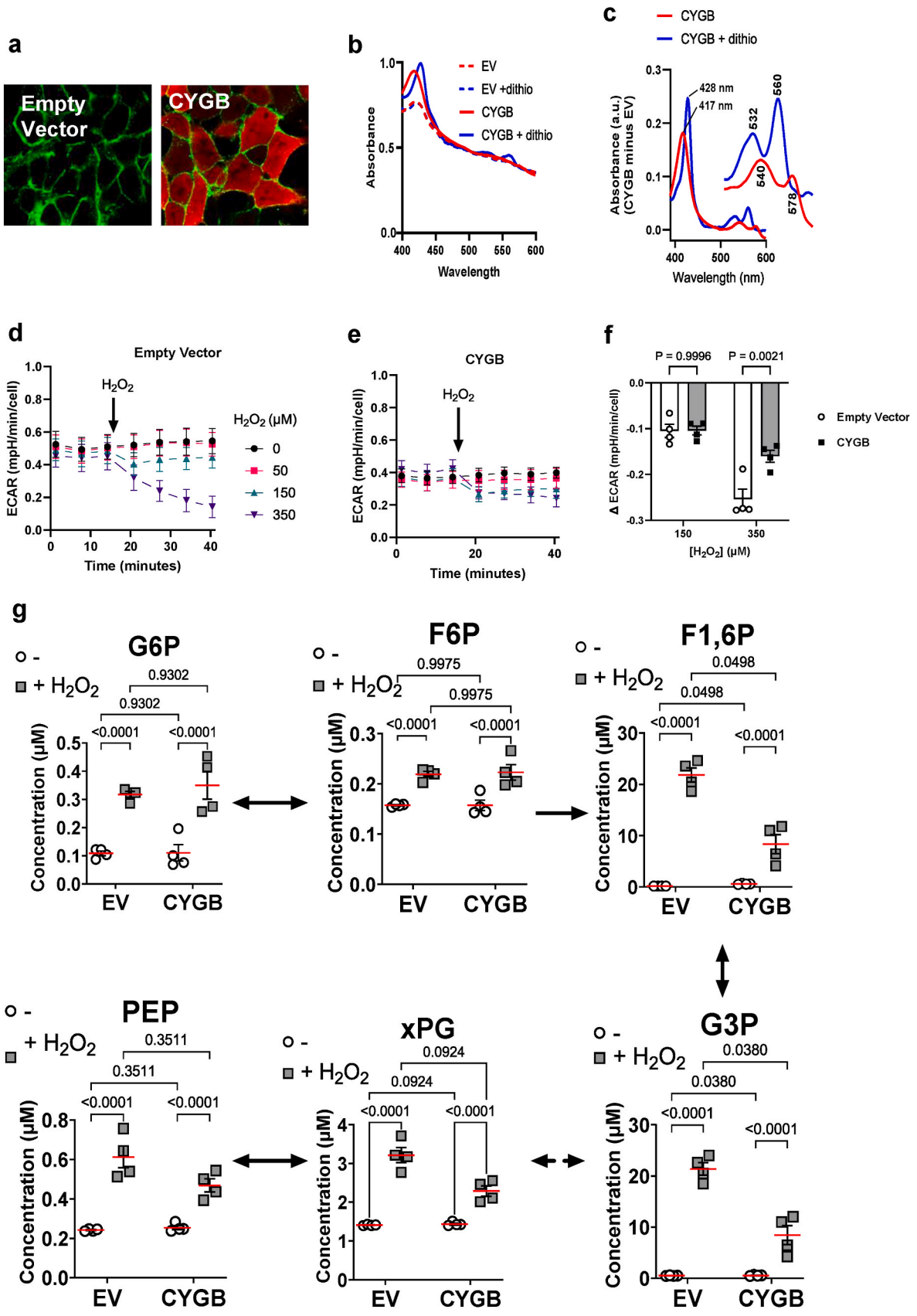

(caption on next page)

Fig. 2. Cytoglobin desensitizes glycolysis from hydrogen peroxide-mediated inhibition in cultured cells. a, Representative indirect immunofluorescence staining for cytoglobin (CYGB; red) from HEK293 cells without (Empty Vector) or with cytoglobin (CYGB) expression. Green staining is a membrane marker to delineate cells. **b**, UV–Vis spectra obtained from live HEK293 cells without (EV) or with cytoglobin (CYGB) expression, in the absence or presence of dithionite (dithio). **c**, CYGB minus EV difference spectra for live HEK293 cells with or without dithionite as shown in panel b. **d** and **e**, Representative tracing of extracellular acidification rate (ECAR) measurements obtained from HEK293 cells without (d, Empty Vector) or with (e, CYGB) cytoglobin expression. Arrows indicate addition of hydrogen peroxide (H_2O_2) at different final concentrations. Each time-point and bar represent the average and standard error for at least 4 wells per time point (technical replicates). **f**, Quantitation of the change in ECAR over time following the addition of hydrogen peroxide (H_2O_2, 150 and 350 μM). Each point represents independent experimental replicates. Statistical analysis was performed using two-way ANOVA with Tukey's multicomparisons test. **g**, Metabolic response of control HEK293 cells (EV = Empty Vector) and HEK293 cells expressing cytoglobin (CYGB) following exposure to 150 μM hydrogen peroxide for 10 min. Concentrations of intracellular glycolytic metabolites were determined by mass spectrometry. Abbreviations: G6P, glucose-6-phosphate; F6P, fructose-6-phosphate; F1, 6P, Fructose-1-6-biphosphate; G3p, Glucose-3-phosphate; xPG, 2/3-phosphoglycerate; PEP, phosphoenolpyruvate. All graphs show mean ± SEM of four independent experimental replicates. Statistical analysis was performed using two-way ANOVA with Tukey's multicomparisons test.

2.2. Expression of cytoglobin decreases the sensitivity of the glycolytic pathway to H_2O_2 in cultured cells

To further confirm the role of cytoglobin in protecting against H_2O_2-mediated inhibition of glycolysis, HEK293 cells were transfected with plasmids to stably express human cytoglobin (hCYGB) or a control plasmid (EV, Empty Vector). The expression of cytoglobin was verified by indirect immunofluorescence (Fig. 2a). We also examined the spectral properties of HEK293 cells expressing cytoglobin using a spectrophotometer equipped with an integrating cavity [29]. Cells expressing cytoglobin showed characteristic spectral features for cytoglobin at the Soret peak with shift of the 417 nm peak to 428 nm following reduction by sodium dithionite (Fig. 2b). In addition, differential spectra between cells with empty vectors and those expressing human cytoglobin revealed primary peaks at 540 and 578 nm, consistent with oxycytoglobin ($CygbFe^{2+}$-O_2; Fig. 2c). Again, reduction of the cell suspension with dithionite led to the formation of deoxycytoglobin with the expected shift at 532 and 560 nm ($CygbFe^{2+}$, Fig. 2c). Interestingly, treatment of cells expressing cytoglobin with cyanide, which binds ferric heme, resulted in spectral changes consistent with the formation of cytoglobin ferric-cyanide heme (Supplementary Fig. 3a.). However, the sequential addition of increasing concentrations of H_2O_2 did not result in any significant changes in the spectral characteristic of intracellular cytoglobin (Supplementary Fig. 3b).

We found that addition of bolus H_2O_2 inhibited the extracellular acidification produced by HEK293 cells with empty vector (Fig. 2d) and cells expressing cytoglobin showed decreased inhibition at the highest concentration of H_2O_2 tested (Fig. 2e and f). To confirm these results, we performed a targeted metabolomic analysis of glycolytic intermediates in cells following exposure to bolus H_2O_2 for 10 min H_2O_2 treatment increased all metabolites concentrations tested, irrespective of cytoglobin expression (Fig. 2g). However, a key feature of the metabolic profile following H_2O_2 treatment, was the accumulation of metabolites directly upstream of GAPDH at much higher concentrations than those immediately downstream of GAPDH (20 μM G3P compared to ~3 μM for xPG with H_2O_2). This was consistent with past studies showing that the reversible oxidative inhibition of GAPDH is a primary determinant of the inhibition of the glycolytic pathway by H_2O_2.[12] This difference was significantly reduced in cells expressing cytoglobin. H_2O_2 treatment also increased levels of ribose-5-phosphate and sedoheptulose-7-phosphate, two intermediates of the pentose monophosphate pathway and this was reversed upon expression of cytoglobin (Supplementary Fig. 4). It is noteworthy that the sensitivity of cells to H_2O_2 was different in the two assays utilized (ECAR vs. metabolomics). This might reflect differences in treatment procedures (96 well format for ECAR compared to larger plate format for the metabolomics). The determination of ECAR is obviously a more global assessment of glycolytic fitness that relies on hydrogen ion production while the metabolomic mass spectrometry measures specific metabolic intermediates. In total, these results showed an attenuation of the inhibitory effect of H_2O_2 on glycolysis by cytoglobin.

2.3. Cysteine and heme requirements for the decomposition of intracellular H_2O_2

To further elucidate the mechanism by which cytoglobin decreases intracellular H_2O_2, we examined the oxidation of the genetically encoded H_2O_2 sensor Hyper7-NES (NES, nuclear exclusion sequence for cytosolic localization, Fig. 3a) [30,31]. We found that baseline values for Hyper7-NES were lower in cytoglobin expressing cells compared to EV controls suggesting a more reduced intracellular environment (Fig. 3b and c). Although this effect could have been produced through quenching of Hyper7 fluorescence by cytoglobin, this possibility could be safely eliminated since only very limited changes were obtained with myoglobin overexpression (Supplementary Fig. 5). Addition of H_2O_2 increased Hyper7-NES oxidation in control and cytoglobin expressing cells (Fig. 3d). Remarkably, cytoglobin expression was also associated with a sharp increase in Hyper7-NES reduction rates compared to control such that approximately 25 min following the addition of H_2O_2, values were returned to baseline (Fig. 3b–d and e). This suggested increased metabolism of intracellular H_2O_2. This was most evident at the 100 and 200 μM final concentrations of H_2O_2 tested (Fig. 3e), with no statistically significant differences at 20 and 50 μM. Independent of cytoglobin expression, decrease in thioredoxin 1 protein levels through siRNA or inhibition of thioredoxin reductase with auranofin inhibited the reduction of Hyper7-NES (Supplementary Fig. 6) in accordance with previous studies[30].

In vitro, cytoglobin ligand binding and reactivity require a functional heme center that is stabilized by a proximal and distal histidine residue [32]. In addition, heme chemistry is allosterically regulated by an intramolecular disulfide bridge between Cys38 and Cys83 [33–38]. Thus, we generated cell lines expressing cytoglobin variants with specific point mutations including H81G, H113G, C38G, and C83G (Fig. 3f). Equal levels of protein expression were confirmed by Western blot except for the double mutant, which was excluded from subsequent experiments (Fig. 3g). Consistent with an essential role for the heme center [19], Hyper7-NES kinetics were restored to those of the control cells lacking cytoglobin following the expression of the H81G (distal histidine residue) or H113G (proximal histidine residue) variants in HEK cells (Fig. 3h). Importantly, while the C38G mutant was functional, the C83G mutant lacked antioxidant activity, (Fig. 3h). To confirm these results, we directly measured the activity of GAPDH. In agreement with the Hyper7 results, the protective effect of cytoglobin on H_2O_2-mediated inhibition of GAPDH was reversed in H81G, H113G, and C83G variants but not C38G (Fig. 3i).

2.4. Cytoglobin inhibits peroxiredoxin hyperoxidation and maintains active peroxiredoxin 2 in cells

A sensitive method to measure changes in intracellular redox state in response to H_2O_2 is by examining the conversion of cytosolic peroxiredoxins to different oxidation states [39]. Briefly, the catalytic cycle of conventional peroxiredoxins consists of the oxidation of a peroxidatic cysteine residue by H_2O_2 to yield the initial sulfenic acid intermediate [40]. This promotes peroxiredoxin homodimerization through

formation of an intermolecular disulfide with a resolving cysteine residue. The disulfides are then reduced by the thioredoxin/thioredoxin reductase system to regenerate the thiolate on the peroxidatic cysteine residues. The catalytic activity of mammalian peroxiredoxins is also accompanied by the progressive oxidation of cysteine sulfenic intermediates to sulfinic and sulfonic acid moieties (termed hyperoxidation), which leads to inactivation of their peroxidase activity [41–43]. We reasoned that if cytoglobin were to promote the degradation of intracellular H_2O_2, it could be competitive with peroxiredoxins.

Hyperoxidation of peroxiredoxins was monitored on Western blots using an antibody directed against stable peroxiredoxin sulfinic and sulfonic residues [44]. We found that cytoglobin expression was associated with a decrease in hyperoxidation following treatment of the cells with H_2O_2 (Fig. 4a). Next, we followed the monomeric/dimeric states of the two primary cytosolic peroxiredoxins, peroxiredoxin 1 and 2. This can be achieved through post-treatment of cells with N-ethylmaleimide (NEM) followed by non-reducing SDS PAGE of the lysates [39]. The monomeric and dimeric forms of the two peroxiredoxins were observed in both control and cytoglobin expressing HEK293 cells (Fig. 4b and c). The high percentage of peroxiredoxin 2 dimers in resting cells compared

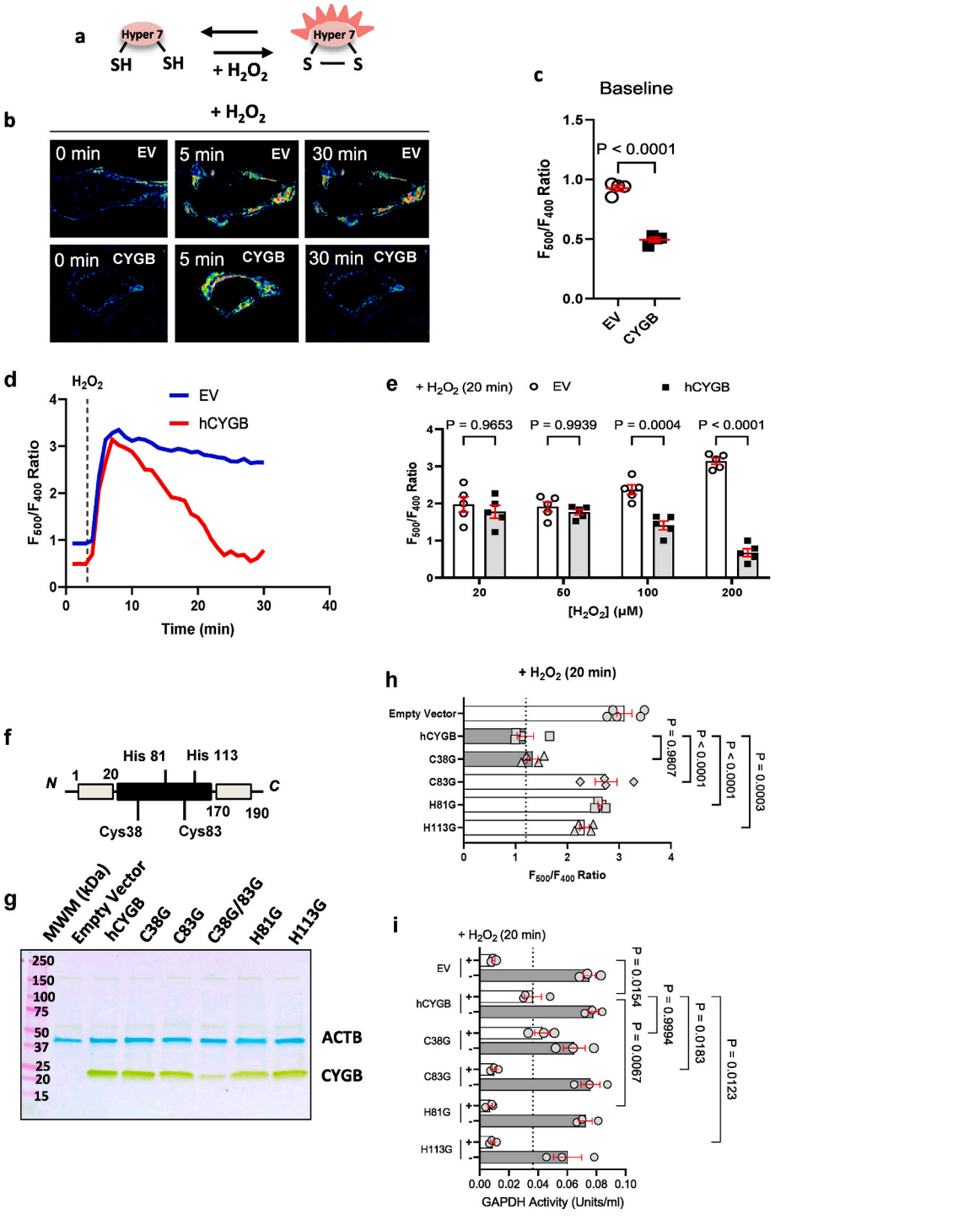

(caption on next page)

Fig. 3. Cytoglobin facilitates the reduction of the cytosolic hydrogen peroxide sensor Hype7-NES. a, The genetically encoded hydrogen peroxide sensor Hyper7 contains two cysteine residues that are reversibly oxidized by hydrogen peroxide, leading to ratiometric changes in fluorescence excitation. **b**, Representative pseudo-color images of the ratiometric measurement of Hyper7 fluorescence in control (EV = Empty Vector) HEK293 cells or cells stably expressing human cytoglobin (CYGB), both with transient expression of Hyper7-NES (NES, nuclear exclusion signal). Pictures were taken just before (0 min), and 5 or 30 min following the addition of 200 μM hydrogen peroxide. One cell is shown for each condition. **c**, Baseline values of ratiometric determination of Hyper7-NES fluorescence. Each data point represents an independent replicate and measurements for 4 to 6 cells were collected for each replicate with bar as mean ± SEM. Statistical analysis was performed using unpaired Student's t-test. **d**, Representative profile of the ratiometric measurement of Hyper7 fluorescence over time in control (EV = Empty Vector) HEK293 cells or cells stably expressing human cytoglobin (CYGB), both with transient expression of Hyper7-NES (NES, nuclear exclusion signal) and treated with bolus hydrogen peroxide (H_2O_2, dashed line). **e**, HEK293 cells with or without cytoglobin expression were treated with different concentrations of hydrogen peroxide and Hyper7 ratiometric changes were recorded over time and quantified at the 20 min time-point. Each point represents an independent experimental replicate with bar as mean ± SEM and two-way ANOVA with Tukey's multicomparisons test. **f**, Schematic of the primary structure of cytoglobin depicting the N- and C-terminal ends, and the position of the proximal (H113) and distal histidine residues (H81), and the two cysteine residues. **g**, Multiplex Western blot analysis of lysates from HEK293 cells stably expressing cytoglobin cysteine and histidine variants using β-actin (gene code ACTB) as an internal reference. **h**, HEK293 cells expressing the cytoglobin variants were transiently transfected with Hyper7-NES followed by treatment with 200 μM hydrogen peroxide. Ratiometric changes were recorded over time and quantified at the 20 min time-point. Each point represents independent experimental replicates with bar as mean ± SEM and one-way ANOVA with Tukey's multicomparisons test. **i**, Control (EV = Empty Vector) and cytoglobin (CYGB) expressing HEK293 cells were exposed to 200 μM hydrogen peroxide for 10 min and lysates were prepared for determination of GAPDH activity. Each point represents independent experimental replicates. Statistical analysis was performed using two-way ANOVA with Tukey's multicomparisons test.

to peroxiredoxin 1 was evident. This could not be attributed to artefactual oxidation of the samples used for peroxiredoxin 2 determination because the Western blots for peroxiredoxin 1 and 2 were generated from the same NEM-treated lysates. This suggested different sensitivity of the two isoforms to basal conditions and possibly preferential activation of peroxiredoxin 2. For these experiments, HEK293 cells were maintained on growth media until treatment with H_2O_2 in serum-free media, possibly favoring continued growth factor-mediated receptor activation and sustained basal H_2O_2 production preferentially sensed by peroxiredoxin 2. This would be in agreement with past work indicating that peroxiredoxin 2 activity responds to lower levels of H_2O_2 than peroxiredoxin 1 [45].

Peroxiredoxin 1 responded to the addition of H_2O_2 with a sharp increase in the dimeric form at 2 min (Fig. 4b). Following the addition of H_2O_2, active dimers in control cells were lost following the addition of H_2O_2 due to progressive hyperoxidation of the monomeric peroxiredoxin [46]. Peroxiredoxin 1 activity was unaffected by cytoglobin expression (Fig. 4b). However, we found that the loss of dimeric peroxiredoxin 2 was delayed in the presence of cytoglobin with the 2 min time-point reaching statistical significance (Fig. 4c). Overall, our results indicate that the antioxidant activity of cytoglobin is sensitive enough to specifically alter peroxiredoxin 2 activity through a decrease in the rate of inactivation of the active dimeric form.

2.5. Peroxidase activity of cytoglobin in vitro

In this last set of experiments, the ability of cytoglobin to compete with peroxiredoxin 2 and to consume H_2O_2 was determined *in vitro* using purified recombinant proteins. First, assessment of protein mobility in non-reducing SDS-PAGE confirmed that recombinant human cytoglobin migrated as two distinct bands that were assigned to monomers with an intramolecular disulfide bridge ($M_{S\text{-}S}$, lower band) or with reduced cysteine residues (M_{SH}, upper band, Supplementary Fig. 7a, **left panel**), as previously described [35]. In accordance, cytoglobin migrated as a single band in reducing gels, just below the 25 kDa molecular weight marker (Supplementary Fig. 7a, **right panel**) while the C38G and C83G variants migrated as single bands under non-reducing and reducing conditions. UV-VIS spectroscopy confirmed that purified recombinant human cytoglobin was present in the ferric state, which was reduced by dithionite to oxyferrous cytoglobin (Supplementary Fig. 7b).

Next, we followed the oxidation of reduced recombinant peroxiredoxin 2 by H_2O_2 in the presence of increasing concentrations of cytoglobin (Fig. 5a). As previously shown by others, Western blotting indicated that pre-reduced recombinant peroxiredoxin 2 consisted of the reduced monomeric subunit at ~22 kDa and homodimer linked by one disulfide bridge (Fig. 5a, upper panel) [47]. The latter band has been shown to be due to the reaction of peroxiredoxin 2 with adventitious H_2O_2 that might be present during the purification process. Importantly, there was no evidence of hyperoxidation in freshly isolated peroxiredoxin 2, based on Western blotting with a primary antibody directed against hyperoxidized peroxiredoxin (Fig. 5a, lower panel). Addition of a 10-fold excess of H_2O_2 (25 μM) to peroxiredoxin 2 promoted the transition of the reduced monomer to the homodimer linked with one or two disulfide bridges. Hyperoxidation of the homodimer with one disulfide bridge was now evident. Significantly, cytoglobin inhibited the hyperoxidation of peroxiredoxin 2 such that addition of a 6-fold excess of cytoglobin almost completely inhibited peroxiredoxin 2 hyperoxidation and the formation of the one-disulfide link homodimer. These results indicated that the reaction of H_2O_2 with cytoglobin is competitive with the hyperoxidation of peroxiredoxin 2. Using the antibody against hyperoxidized peroxiredoxin, we also observed a band at 25 kDa, which we attributed to cross-reactivity of the antibody with oxidized cytoglobin since the peroxiredoxin 2 monomer disappears with H_2O_2 addition.

Finally, we used the ferrous oxidation xylenol assay [48] to compare the rates of H_2O_2 degradation by recombinant cytoglobin and peroxiredoxin 2, as described by Kang et al. [49]. We found that cytoglobin (2.5 μM final concentration) promoted the decomposition of H_2O_2 (25 μM; Fig. 5b) at rates that were comparable to human peroxiredoxin 2 (2.5 μM final concentration). The reducing agent DTT was included as an electron donor to maintain the activity of peroxiredoxin 2. Cytoglobin activity did not require DTT (Fig. 5b) and was inhibited by treatment with cyanide, a ligand to ferric cytoglobin (Fig. 5c). We found that the C83G mutant decomposed H_2O_2 at a rate slower than the wildtype protein (Fig. 5d) but the C38G mutant was indistinguishable from the wildtype. Lastly, another proposed activity for cytoglobin is superoxide scavenging [18]. However, additional experiments to evaluate superoxide dismutation by purified human cytoglobin failed to detect any superoxide dismutase activity compared to SOD1 (Supplementary Fig. 7 c-f), consistent with other studies [50,51].

3. Discussion

The protection afforded by cytoglobin against the cytotoxic and profibrotic effects of H_2O_2 has been documented extensively following initial demonstration that cytoglobin has significant peroxidase activity [16,52–59]. However, later work determined that the second order rate constant for the reaction of cytoglobin with large excess of H_2O_2 was ~300 M^{-1} s^{-1} [19]. This is several orders of magnitude slower than the reaction of H_2O_2 with conventional intracellular heme and thiol-based peroxidases [47]. This specific result argued against a direct role for cytoglobin as a physiologically relevant H_2O_2 scavenger. In the present study, we carefully reassessed the ability of cytoglobin to consume H_2O_2. We show that cytoglobin decomposes H_2O_2 at rates comparable to

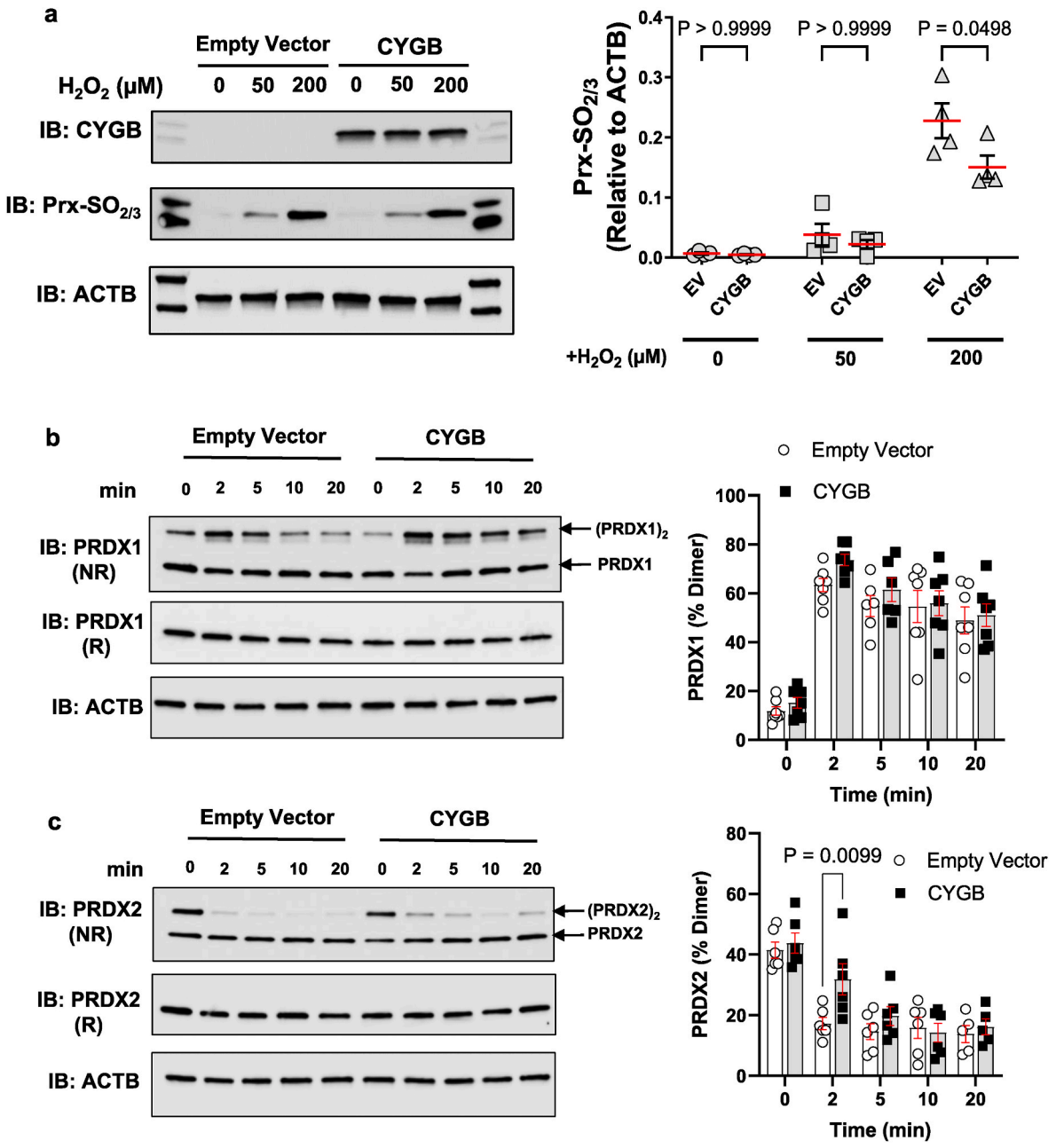

Fig. 4. Cytoglobin decreases peroxiredoxin hyperoxidation and maintains active peroxiredoxin 2. a, Control (Empty Vector) and cytoglobin (CYGB) expressing HEK293 cells were exposed to hydrogen peroxide for 10 min followed by the addition of NEM. Lysates were used for non-reducing SDS PAGE and Western blotting to examine protein levels of hyperoxidized peroxiredoxins (Prx-SO2/3) using beta actin (ACTB) as an internal reference. Cytoglobin levels (CYGB) are also shown. Right panel, quantitation of experiments described in left panel. **b** and **c**, Control (Empty Vector) and cytoglobin (CYGB) expressing HEK293 cells were exposed to 150 μM hydrogen peroxide for various amounts of time followed by the addition of NEM. Lysates were used in reducing and non-reducing SDS PAGE and Western blotting to examine protein levels of peroxiredoxin 1 (b, PRXD1) and 2 (c, PRXD2). Arrows indicate the position of the dimers and monomers. Right panels, quantitation of experiments represented in left panels. All graphs show mean ± SEM and each point represents one independent experimental replicate. Statistical analysis was performed using two-way ANOVA with Tukey's multicomparisons test.

that of the thiol-peroxidase peroxiredoxin 2 and that it competitively inhibits peroxiredoxin 2 hyperoxidation. We show that cytoglobin counteracts the H_2O_2-mediated re-routing of glycolysis towards the pentose monophosphate pathway in cells and isolated mouse arteries. The antioxidant activity of cytoglobin requires one of the two surface cysteine residues (C83), in addition to the heme center. Overall, our results support a role for cytoglobin as a physiological target of H_2O_2 and possible regulator of H_2O_2 redox signaling.

The expression of cytoglobin in vascular cells has been documented in both rodent and human vessels [15,60–62]. Immunofluorescent studies have shown association of cytoglobin protein immunoreactivity with the medial layer of rat and mouse vessels including the aorta, carotid, and mesentery [15,63]. The present work indicates that cytoglobin is by far the most abundant globin transcript in mouse carotid arteries. Moreover, we used a smooth muscle lineage tracing mouse line to assert cytoglobin protein expression in medial vascular smooth muscle cells. However, our results also indicate that cytoglobin co-associates with adventitial cells in mouse vessels including adventitial fibroblasts, based on co-association of cytoglobin with cells that express dermatopontin, a fibroblast marker [28]. Past studies suggest

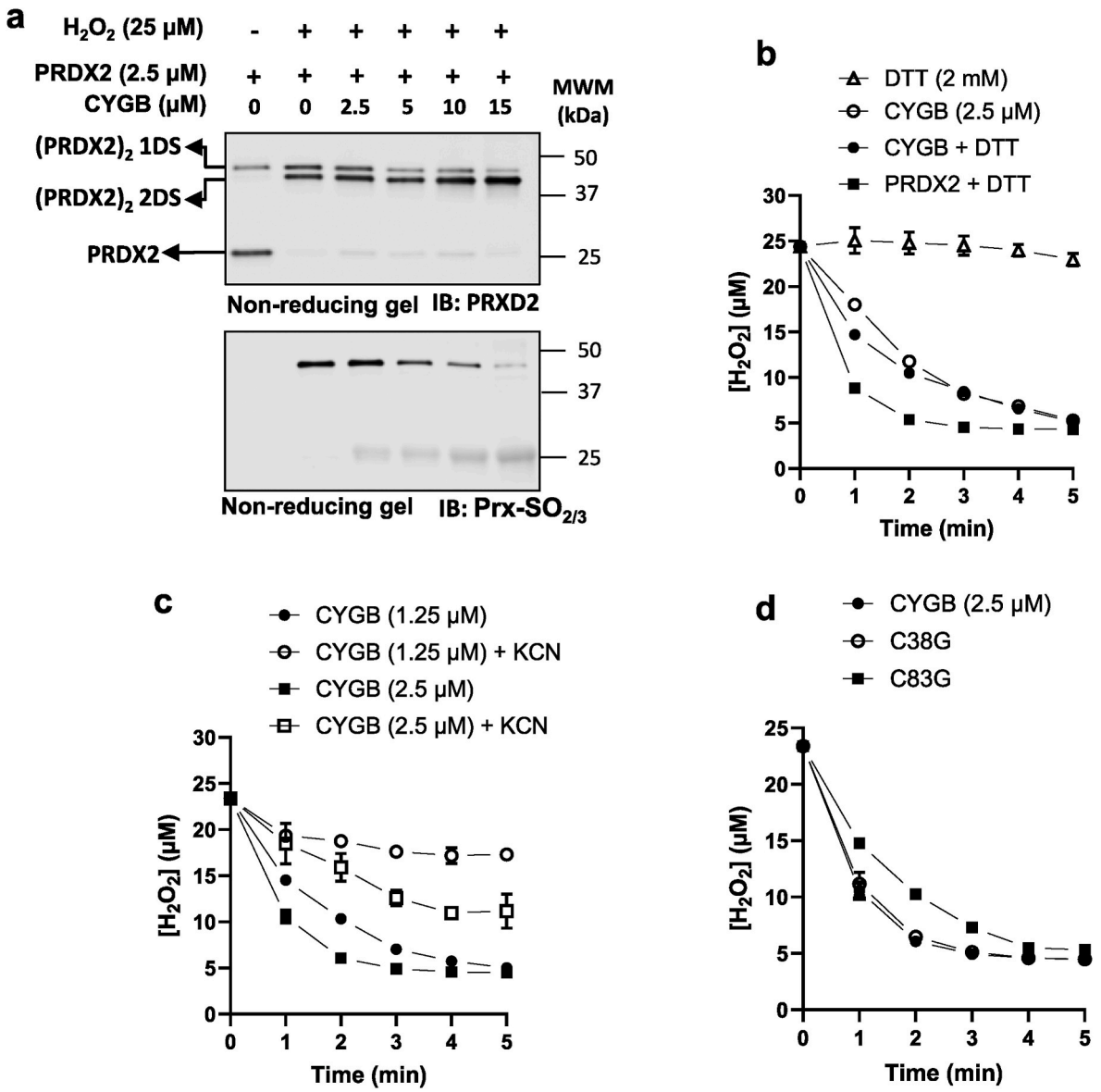

Fig. 5. The peroxidase activity of cytoglobin is competitive with peroxiredoxin 2 hyperoxidation ***in vitro***. **a**, Non-reducing SDS-PAGE gels of reduced peroxiredoxin 2 (2.5 μM) incubated with hydrogen peroxide (H_2O_2, 25 μM) for 5 min in the presence of increasing concentrations of cytoglobin. Representative of three independent experiments. **b**, Time-dependent decomposition of hydrogen peroxide (25 μM) by cytoglobin (CYGB; 2.5 μM) or peroxiredoxin 2 (PRDX2; 2.5 μM) with DTPA (100 μM) and 100 mM phosphate buffer, in the presence or absence of DTT (2 mM). The reduction of hydrogen peroxide in the presence of DTT alone is also shown. **c**, Effect of potassium cyanide (KCN; 100 μM) on the decomposition of hydrogen peroxide (25 μM) by cytoglobin (1.25 and 2.5 μM). **d**, Peroxidase activity of WT, C38G, and C83G cytoglobin (1.25 μM each) with 25 μM hydrogen peroxide. Results are means of triplicates.

that cytoglobin plays anti-fibrotic functions in the liver and kidney and regulates extracellular matrix deposition by fibroblasts [53,56,64–67]. The role of cytoglobin in regulating perivascular fibrosis has yet to be determined but our findings clearly provide support for further investigation.

The H_2O_2-mediated re-routing of the glycolytic pathway towards the pentose monophosphate pathway is an important cellular mechanism that regulates the provision of reducing equivalents in response to changes in intracellular H_2O_2 concentrations [12,13,24,25,68]. We found that carotid arteries isolated from cytoglobin global knockout mice were more sensitive to H_2O_2 challenge. This is important because it indicates that the amount of cytoglobin expressed in vessels was sufficient to contribute to H_2O_2 decomposition. Consistent with these results, we showed that the expression of cytoglobin in cultured cells promoted glycolysis in the presence of exogenous H_2O_2. Although there might exist several mechanisms of how glycolysis inhibition is achieved through H_2O_2, past studies indicate that the oxidative inactivation of GAPDH is an important component [12,13]. Our metabolomic studies confirmed the increase in glycolytic intermediates following treatment with H_2O_2 and inactivation of GAPDH was reflected by the 5 to 7-fold difference in concentrations between glyceraldehyde 3-phosphate and 1,3 biphosphoglycerate, the reaction intermediates of GAPDH activity. Reversal of effect by cytoglobin was documented not only based on the metabolomic analysis but also by directly measuring GAPDH activity. Mechanistically, our results also suggest major differences between C38 and C83 in their contribution to cytoglobin activity against H_2O_2. In cells, the C83G mutation had strong inhibitory effects, based on the oxidation of the H_2O_2 detector Hyper-7 and inhibition of GAPDH activity. This would suggest a unique mechanism in which C83 would play an important role in regulating cytoglobin activity, independent of the formation of an intramolecular disulfide bridge as previously demonstrated *in vitro* [35,36,38].

In light of the sensitivity of GAPDH and Hyper-7 to cytoglobin, we considered whether intracellular cytoglobin could alter the redox state of peroxiredoxin 1 and 2, two important thiol-based peroxidases that function in H_2O_2 detoxification in the cytosol [69]. We found that the ectopic expression of cytoglobin delayed the oxidative inactivation of peroxiredoxin 2 following bolus addition of hydrogen peroxide, indicating that cytoglobin could compete with the hyperoxidation of peroxiredoxin 2 under these conditions. The observation that cytoglobin did not affect peroxiredoxin 1 activity is more difficult to interpret. These peroxiredoxins share similar structure and catalytic steps. However, peroxiredoxin 2 activity responds to lower levels of H_2O_2 than peroxiredoxin 1 [45] and the rate of disulfide bond formation for peroxiredoxin 2 is ten-fold slower than for peroxiredoxin 1 [45,70]. This may facilitate competition between cytoglobin and peroxiredoxin 2 for reaction with H_2O_2 and inhibition of peroxiredoxin 2 hyperoxidation by cytoglobin. We did not explore whether cytoglobin can modify the activity of other intracellular antioxidants such as catalase or the glutathione peroxidases. Kinetic studies have shown that catalase is likely involved in the decomposition of relatively high concentrations of H_2O_2 [71,72]. In contrast glutathione peroxidase activities – like the peroxiredoxins - are saturated at much lower concentrations [71,72]. Thus, a more detailed biochemical and cellular characterization of cytoglobin antioxidant activity will be required to determine how it may affect intracellular H_2O_2 or the extent to which its function as a target of H_2O_2 may be affected by other intracellular antioxidants.

In vitro, we found that the rate of H_2O_2 decomposition by cytoglobin was comparable to that of peroxiredoxin 2 (with DTT as the reductant), suggesting a much faster reaction than previously thought. Overall, the sensitivity of the reaction to KCN indicates a heme-based mechanism like the one described for hemoglobin and myoglobin in which ferryl heme is formed following reaction with H_2O_2 [73–76]. The formation of such intermediates has been observed for cytoglobin [19] and the reduction step required for the catalytic activity of purified cytoglobin might occur through reaction with buffer components [77]. However, this does not account for the contribution of C83 to H_2O_2 removal, although the effect was much smaller with purified cytoglobin than in cells. The formation of a disulfide bridge between C38 and C83 can be excluded because the C38 mutant was as active as the wild type cytoglobin. The fact that DTT had no effect on the antioxidant activity of purified cytoglobin suggests that C83 might be directly oxidized to the sulfinic acid ($-SO_2H$) that is insensitive to reduction by DTT. DeMartino et al. previously found that half of the cytoglobin thiol content was unavailable for disulfide formation after H_2O_2 treatment in oxygenated solutions [38]. They further proposed that the hyperoxidation of at least one of the two cysteines occurred [38]. Altogether, these results indicate two important sites for the reaction of cytoglobin with H_2O_2, the heme center and C83. Whether the reactions at these two sites occur independently or involve coordinated electron transfer from the heme center to C83 will need to be clarified in future studies.

In summary, our results suggest that cytoglobin stands out against other mammalian globins due to its higher reactivity for H_2O_2. A second order rate close to that of peroxiredoxin 2 hyperoxidation (12 000 M^{-1} s^{-1}) [41] is proposed based on our competition experiments (Fig. 5). This suggests that cytoglobin plays a significant role in H_2O_2 -mediated redox signaling through direct sensing of intracellular H_2O_2. It is important to note that the intracellular concentration of cytoglobin is likely to be much lower than peroxiredoxin 2 in native systems, including in vessels. This suggests that the antioxidant activity of cytoglobin might require specific molecular interactions and subcellular associations that may facilitate its effect on peroxiredoxin 2 or even on GAPDH. In support, analysis of cytoglobin protein interactome by immunoprecipitation and mass spectrometry identified peroxiredoxin 2 as a protein interactor, while peroxiredoxin 1was absent from this dataset [16]. Previously, we showed that cytoglobin is actively translocated to the nucleus through a redox signal initiated by serum stimulation and driven by the NADPH oxidase NOX4 [16] in human vascular smooth muscle cells. This could be recapitulated in the absence of serum through exogenous addition of H_2O_2[16]. We propose that defining the specific role of the cytoglobin/H_2O_2 reaction in promoting cytoglobin nuclear translocation and downstream signals will be key to understanding cytoglobin's functions in the vasculature and elsewhere.

4. Materials and methods

4.1. Supplies and reagents

All supplies and reagents are listed in Supplementary Table 1.

4.2. Mice

All procedures related to mice were approved by the Institutional Animal Care and Use Committee at Albany Medical College. The cytoglobin "knock out first" allele was obtained from the University of Toronto, Canada, and global wild-type and cytoglobin knockout mice littermates (Cygb WT mice and Cygb KO) were generated from heterozygous breeding pairs. Both males and females were used and randomly assigned to experimental groups. Myh11-Cre^{ERT} was a kind gift from Dr. Singer (Albany Medical Center) and ROSA26-zsGreen reporter mice were obtained from the Jackson Laboratory. Myh11-Cre^{ERT} transgenic mice and ROSA26-zsGreen were bred to generate tamoxifen-inducible SMC-specific zsGreen reporter mice. ZsGreen expression is induced in mice by administering 2 mg tamoxifen for 5 days by peritoneal injection. Mice were housed in pathogen-free rooms with controlled light-dark cycle, temperature, and humidity. Mice were kept in cages in groups of five or fewer with ad libitum access to food and water. Eight-to thirteen-week-old mice were euthanized and the thoracic aorta, left common carotid artery, heart, liver and spleen were collected for immunoblotting, imaging, and metabolic flux studies.Mouse genotypes were confirmed with PCR. Briefly, tail snips were digested with DirectPCR (tail) reagent supplemented with Proteinase K from Viagen. PCR was run with GoTaq G2 mastermix on a BioRad Mycycler thermocycler.

4.3. Generation of HEK 293 clones, cell culture, and treatment with hydrogen peroxide

A pcDNA 3.1 plasmid containing the full length human cytoglobin gene was purchased from GenScript. The empty vector control and specific point mutations of this plasmid were also generated by GenScript. Plasmids were transformed with Invitrogen's One Shot Top10 chemically competent cells, streaked onto LB agar plates with ampicillin selection and incubated overnight at 37°C to achieve colonies. Individual colonies were selected and cultured overnight in 5 mls aliquots of LB broth containing 100 μg/ml Ampicillin. The overnight cultures were used to inoculate fresh LB broth containing 100 μg/ml Ampicillin and incubated at 37°C with shaking overnight. Plasmid DNA was recovered from the LB broth with a Machery-Nagel NucleoBond Xtra Midi plus kit as per their protocol. HEK293 cells were transfected with Dharmafect kb; stably expressing human Cytoglobin cell lines were established through limiting dilution cloning. Cells were maintained in DMEM supplemented with 10 % fetal calf serum, 2 mM L-glutamine, and 750 μg/ml Geneticin for selection.

For most experiments using adherent HEK 293 clones, one million cells were seeded in 60 mm dishes containing four mls of DMEM supplemented as above. Forty-eight hours post seeding the growth media was replaced with 4 mls of serum free media and cells were treated with 20–200 μM H_2O_2 for 2–20 min. For Seahorse experiments cells were seeded into poly-L lysine coated 96 well flux plates at a density of 1×10^4 cells/well in 10 % media as described above. Cells were returned to the incubator for 48 h. One hour prior to experimentation the growth media was replaced with seahorse XF media supplemented with 10 mM glucose and cells were equilibrated without CO_2 buffering at 37°C for 1

h. Each measurement included 3 min mix and 3 min measure for 3 rounds.

4.4. Generation of recombinant human cytoglobin and recombinant human peroxiredoxin 2

pET-28a(+) HIS tagged plasmids for human cytoglobin,C38G mutant,C83G mutant and peroxiredoxin 2 were acquired from Genscript. Plasmids were transformed with Invitrogen's BL21 chemically competent E-coli cells, streaked onto LB agar plates with 50 μg/ml kanamycin and incubated overnight at 37°C to generate individual colonies. Well defined colonies were selected and cultured overnight in 5 mls aliquots of LB broth containing 50 μg/ml Kanamycin. The overnight cultures were used to inoculate fresh LB/Kanamycin broth to an OD600 between 0.05 and 0.1, these expanded cultures were returned to the incubator until they reached mid log phase OD600–0.4 (2–3 h). At this point, protein expression was induced by the addition of 0.5 mM IPTG. To enhance cytoglobin expression 500 μM 5-aminolevulinic acid hydrochloride (ALA) a precursor for heme biosynthesis was also added to each cytoglobin samples. The cultures were incubated for an additional 12–18 h at room temperature prior to collection of bacterial pellets by centrifugation at 10 000 x G for 15 min at 4°C. The recombinant proteins were purified with a Thermo Scientific HisPur Ni-NTA Purificaton kit as per manufacturer's instructions. Proteins were desalted with Zeba Spin Desalting/Buffer Exchange columns following the manufacturer instructions, working aliquots were snap frozen in liquid nitrogen and stored at −80°C.

4.5. Spectrophotometric analysis of cytoglobin in cells

Spectral analysis of cytoglobin in HEK293 clones was performed as previously described with some modifications [78]. Briefly, absorbance spectra of whole cell suspensions from 1×10^6 to 1×10^7 cells/ml were read using an Olis-Clarity VF spectrophotometer with an eight-ml cuvette. Apparent absorbance values were recorded relative to a buffer baseline. Live cell spectra were recorded before and after the addition of 2.5 mM dithionite, 125, 250 and 500 μM hydrogen peroxide, or 100 μM potassium cyanide. Spectra subtraction between cells with empty vector and cells expressing cytoglobin was performed using Olis software and plotted using Graph Pad Prism v9.

4.6. Transcriptomic analysis

RNA was quantified using a Qubit RNA HS Assay kit and Flex Fluorometer. Library preparation was performed using an Ion Chef System followed by sequencing using an Ion GeneStudio S5 Plus System both following manufacturer's suggested protocols for the Ion AmpliSeq Transcriptome Mouse Gene Expression Kit for mouse left common carotid artery or Ion AmpliSeq Transcriptome Human Gene Expression Kit for HEK293 cells (All from Thermo Fisher Scientific, San Jose, CA).

4.7. Reducing and non-reducing immunoblotting

After adherent HEK 293 clones were treated with hydrogen peroxide for the specified times, 50 mM NEM was added to each plate and incubated for 2 min at RT. Media was aspirated and each plate was washed with 1 ml of 50 mM NEM in DPBS. Cells were lysed in 500 μL of RIPA buffer supplemented with 50 mM NEM and HALT protease/phosphatase inhibitors (1:100). Lysates were spun at 12 000 x G for 20 min at 4°C. The cleared supernatants were transferred to fresh tubes prior to protein quantification with the Pierce BCA protein assay. Samples were divided into two; one received an equal volume of 2X SDS sample buffer with 720 mM β-mercaptoethanol (reducing) and the other 2X SDS-sample buffer without β-mercaptoethanol (non-reducing); samples were heated to 95°C for 5 min. Equal amounts of total protein were electrophoresed on 4–20 % gradient gels until the dye front reached the bottom. Proteins were transferred to PVDF membranes at 100 V for 1 h. Membranes were blocked overnight with 5 % NFM/TBST at 4°C. Blots were incubated with primary antibodies for PRX-$SO_{2/3}$ (1:1500), PRDX1(1:10 000), PRDX2 (1:10 000) or CYGB (1:2000) for 1 h at room temperature, washed 3 × 15 min, incubated with either goat anti mouse or goat anti rabbit-HRP secondary antibodies (1:2500) for 1 h at RT, washed 3 × 15 min, then visualized using BioRad Clarity Western ECL substrate on a BioRad ChemiDoc MP imaging system. Blots were rinsed with tap water then washed again and re-probed with an anti-β-Actin peroxidase antibody (1:25 000) for 30 min at room temperature, after a final set of washes blots were visualized as before.

4.8. Multiplex immunoblotting

Reduced, untreated cell lysates were prepared in RIPA/HALT lysis buffer, electrophoreses and transferred as outlined above with one exception, the regular PVDF membrane was replaced with low fluorescent PVDF membrane. After overnight blocking in 5 % non-fat milk/TBST the blots were incubated with anti-rabbit Cytoglobin (1:2000) for 1 h at room temperature, washed 3 × 15 min in TBST. Incubated with a cocktail of the secondary goat anti rabbit StarBright Blue 700 antibody (1:3000) and anti-Actin hFAB Rho (1:3000) for 1 h at room temperature, washed 3 × 15 min in TBST, allowed to dry and imaged with the BioRad ChemiDoc MP imaging system using the Multi Red Blue and Green program.

4.9. Metabolic flux studies and GAPDH activity

Ex vivo studies of metabolic fluxes in isolated vessels were performed as previously described with some modifications [79]. Briefly, the left common carotid arteries were collected from 8 to 13 weeks old CYGB WT and KO mouse littermates after perfusion with PBS under isoflurane anesthesia. The carotid arteries were cleared of exterior fat under a dissecting microscope and cut into two mm sections. Individual wells of XF96 culture plates precoated with CELL-TAK were loaded with 180 μL of XF Base Media containing 10 mM glucose pH 7.4 then equilibrated for 1 h at 37°C in an incubator without CO_2 buffering. The 2 mm carotid artery sections were placed in the wells and briefly spun at 500 rpm for 30 s to adhere vessels to the bottom of the wells. Test compounds were loaded into the corresponding ports of the Sensor cartridge prior to instrument calibration. Acidification rates were measured on a SeaHorse XFe96 analyzer (Agilent Technologies). Titration experiments were performed to establish the optimal dosage H_2O_2 (200 μM), FCCP (1 μM), and the rotenone/antimycin A mixture (0.5 μM). We found that oligomycin did not provide reproducible results, most likely due to limited penetrance. Each extracellular acidification rate measurement included 3 min of mixing, 3 min wait time, and 3 min of continuous measurement with at least three measurement rounds per injection. Following the measurements, images of each vessel were taken for determination of vessel length to normalize ECAR data to vessel surface area. For each experiment, at least two 2-mm pieces were used per mouse and averaged. Biological replicates were individual mice, both males and females were used for these experiments.

For adherent HEK 293 clones the growth media was replaced with seahorse XF media supplemented with 10 mM glucose and cells were equilibrated without CO_2 buffering at 37°C for 1 h. Basline measurements included 3 rounds of 3 min of mixing and 3 min of continuous measurements, this cycle was increased to 4 rounds after injection of 0, 50, 150 and 300 μM H_2O_2.

GAPDH was measured with a GAPDH Activity Assay kit from Sigma Aldrich according to manufacturer's instructions. Briefly, the HEK 293 clones including EV, hCYGB, C38G, C83G, HIS81G and HIS113G were seeded into 60 mm culture plates at a density of 1×10^6 and cultured under selection for 48 h. Cells were harvested and counted. 1×10^6 cells were homogenized in 100 μL of ice cold GAPDH assay buffer, incubated on ice for 10 min, insoluble material was removed by centrifugation at

10 000 x G for 5 min at 4°C. The resulting supernatant was assayed for GAPDH activity according to kit directions. The absorbance was recorded at 450 nm for 10–60 min at 37°C on a Cytation 5 plate reader (Agilent Technologies).

4.10. Metabolomics mass spectrometry analysis

Methods were performed as described previously [80]. Briefly, snap frozen cell pellet samples were kept in the −80 °C freezer until time of extraction. To extract metabolites, samples were extracted with 1 ml of a chilled 40:40:20 ACN:MeOH:water. Samples were lysed by sonication for 20 s at 4 °C, then centrifuged at 4 °C for 2 min at a speed of 14 000 x G. Then 200 μL of the supernatant from each tube was transferred into a low volume amber borosilicate glass autosampler vial with tapered insert and dried by vacuum concentrator. Samples were resuspended in 100 μL of water for LC-MS/MS analysis. A mixture of standards was prepared at 12 concentrations and used for quantification.

For each sample, 10 μL was loaded onto an IonPac AS-11 HC strong anion-exchange analytical column (2 mm × 250 mm, 4 μm particle diameter, Thermo Scientific) with AG-11 HC guard column (2 mm × 50 mm) heated to 40 °C. An Ultimate (Thermo) LC system was used for applying a 0.35 ml/min gradient of mobile phase A (Water, degassed) and mobile phase B (100 mM NaOH, degassed): hold 12.5 % B for 5 min, increase to 20 % over 5 min, increase to 27.5 B over 7.5 min, increase to 42.5 % B over 5 min increase to 95 % B over 10 min, hold at 95 % B for 9.5 min, then returning to 12.5 % B over 0.5 min. Post column eluent was passed through a 2 mm AERS 500e suppressor operated via a reagent-free controller (RFC-10, Dionex) set to 50 mA, a binary pump (Agilent 1100) was used to deliver water at 0.5 ml/min for external water regeneration mode. Then eluent was ionized by electrospray ionization to be analyzed by a TSQ Quantiva mass spectrometer (Thermo Scientific). The following source settings were used: 350 °C vaporization temperature, 350 °C ion transfer tube temperature, 18 units Sheath Gas, 4 unit Aux Gas, 1 unit Sweep gas, polarity switching | 3800 V| (1.5–45 min), and Use Calibrated RF Lens option. MS was operated in single reaction monitoring mode with specified transitions, retention time windows and collisions energies, using 0.7 FWHM resolution for Q1 and 1.2 FWHM for Q3, 0.8 s cycle time, 1.5 mTorr CID gas, and 30 s Chrom Filter. Raw files were processed using Xcalibur Quan Browser (v4.0.27.10, Thermo Scientific); The prepared mixture of standards was used to locate appropriate peaks for peak areas analysis.

4.11. Real-time imaging

HEK 293 cells expressing human cytoglobin or empty vector were seeded between 2×10^3 and 4×10^3 into poly-L-lysine coated 35 mm MatTek glass bottom culture dishes with antibiotic free DMEM supplemented with 10 % Fetal Calf Serum and 2 mM L-Glutamine. Cells were transfected with the pCS2+Hyper7 plasmid using Dharmafect kb transfection reagent according to the manufacturer's recommendations. Twenty-four hours post-transfection, culture medium was replaced with 1.2 ml of HBSS supplemented with 20 mM HEPES. For some experiments, cells were pre-treated with 10 μM final concentration auranofin for 30 min prior to HyPer7 analysis. The 1 mM Auranofin stock was prepared in 100 % EtOH. For other experiments, cells were transiently transfected with the small interfering RNA (siRNA) oligonucleotide against Thioredoxin 1 or a nontarget control using Dharmafect1 according to manufactures recommendations. The cells were silenced for 48 h in Opti-MEM supplemented with 5 % fetal bovine serum prior to a 24 h transfection with the Hyper7 NES as outlined above. Cell imaging was performed using a Leica DMI 8 Thunder microscope, equipped with an HC PL APO 63×1.4NA oil objective at 37 °C. Samples were excited sequentially via 440/15 and 510/15 band-pass excitation filters. Emission was collected every 20 s using a 519/25 bandpass emission filter. After 5–10 images were acquired, a small volume of hydrogen peroxide was carefully added to obtain a final concentration of 200 μM. The time series were analyzed via Fiji freeware (https://fiji.sc). The background was subtracted from 440 to 510 nm stacks. Every 510 nm stack was divided by the corresponding 440 nm stack frame-by-frame. The resulting stack was depicted in pseudo-colors using a "16-colors" lookup table. The Plasmid pCS2+HyPER7-NES was a gift from Vsevolod Belousov (Addgene plasmid # 136 467; http://n2t.net/addgene:136467; RRID:Addgene_136 467).

4.12. Real time PCR

To confirm silencing of Thioredoxin 1 in the real time imaging experiments (Supplementary Fig. 6), HEK 293 cells expressing cytoglobin or empty vector were seeded into standard 35 mm dishes at 5×10^4. Briefly, cells were transiently transfected with siTXN or Scr (non-target control) according to the dharmafect1 protocol. Seventy-two hours post silencing the cells were collected into 1 ml of TRIzol reagent, total RNA was isolated according to standard protocol. Reverse transcription was carried out with a QuantiTect Reverse Transcriptase kit as per package instructions. qPCR was run with SsoAdvanced Universal SYBR Green supermix on a BioRad CFX Connect Real Time System. Gene specific primers; human TXN sense: 5′-CTT GGA CGC TGC AGG TGA TA-3′ and antisense 5′-AGC AAC ATC ATG AAA GAA AGG CT-3'. Human RPS18 was used as the house keeping gene to determine relative expression of Thioredoxin 1. Sense 5′-ATG GGC GGC GGA AAA TAG C-3 and antisense 5′-TCT TGG TGA GGT CAA TGT CTG C-3'.

4.13. Immunofluorescence

For tissues, 10 μm tissue sections were cut from prepared OCT blocks using a Leica CM1850 cryostat and transferred to charged microscope slides, dried at room temperature and stored at −80°c. Slides were removed from the freezer, air dried, fixed with ice cold acetone for 10 min then dried again. After outlining the sections with a hydrophobic barrier pen, they were briefly rehydrated with PBS and blocked with 5 % sera representing the secondary antibody species for at least 1 h. Blocked tissues were incubated with either cytoglobin primary antibody (PTG Lab 1:100) or a matched isotype control for 1 h at room temperature, washed in PBST, then with Goat anti Rabbit AlexaFluor 594 or 647 secondary antibody (1:200) for 1 h at room temperature. Slides were washed once with PBST once with a 50:50 PBS/water mix then stained with 1 μM DAPI for 15 min at room temperature. After a final rinse in the 50:50 PBS/water mixture they were cover slipped with VectaShield Antifade Mounting Medium; sealed with clear nail polish and stored protected from light at 4°C.

For cellular immunofluorescence studies, cells were plated in poly-L-lysine coated 8 well glass bottom Ibidi slides with 400 μL of DMEM supplemented with 10 % FBS and 2 mM L-glutamine then returned to 37°C CO_2 incubator to attach overnight. Cells were fixed in 4 % formaldehyde for 15 min at room temperature washed with PBS then permeabilized in PBS/0.2 % Triton-X100 for 5 min at room temperature, blocked with 5 % serum representing the secondary antibody for at least 1 h. Rabbit anti-cytoglobin primary antibody (PTG Lab 1:200) or a matched isotype control was added for 1 h at room temperature, washed again in PBST, incubated with Goat anti Rabbit AlexaFluor 594 secondary antibody (1:200) for 1 h at room temperature, washed once with PBST, once with a 50:50 PBS/water mix then stained with 1 μM DAPI for 15 min. After one final wash in the 50:50 mixture the slides were cover slipped using VectaShield Antifade Mounting media, sealed with clear nail polish and stored at 4°C in the dark until imaging.

Fluorescence in situ hybridization staining for dermatopontin transcripts was performed using Advanced Cell Diagnostics RNAscope™ Multiplex Fluorescent V2 Assay with the Mm-Dpt probe (catalog 56 429) the positive control probe Mm-Ppib (catalog 313 911) and the negative control probe DapB (catalog 310 043) using the standard protocol. Following completion of the in-situ hybridization protocol, sections were then stained for Cygb (as above).

4.14. Peroxidase and superoxide dismutase activity assays

Hydrogen peroxide degradation was measured in triplicate with a Quantitative Peroxide Assay kit from Pierce following the manufactures protocol. A standard curve of H_2O_2 ranging from 0 to 50 μM was prepared fresh for each experiment in 100 mM Phosphate buffer with 100 μM DTPA. 20 μL of each standard were added in triplicate to the corresponding wells of a 96 well plate. Recombinant human Cytoglobin, C38G, C83G or Peroxiredoxin 2 proteins were diluted to a final concentration of 1.25 or 2.5 μM in 100 mM Phosphate buffer containing 100 μM DTPA. Where noted, 2 mM DTT or 100 μM cyanide were added to the phosphate/DTPA buffer prior to diluting the protein. 18 μL of the 2.5 μM protein sample were added to the corresponding wells on a flat bottom 96 well plate. To begin the time course 2 μL of 250 μM H_2O_2 were added to the 5-min samples followed by the 4-, 3-, 2-, and 1-min samples. At time 0, 200 μL of working reagent was quickly added to all the wells with a multichannel pipet, samples were incubated for 20 min at room temperature and read at 595 nm on a Cytation 5 (Agilent Technologies). 25 μM samples of H_2O_2 were included as a positive control and phosphate/DTPA buffer was used as the blank. After subtracting the blank from all standards and samples, the hydrogen peroxide concentrations were extrapolated from the prepared stand curve.

The superoxide dismutase activity of recombinant cytoglobin was determined by following the reduction of 50 μM ferricytochrome c at 550 nm using a Shimadzu UV-1601 PC spectrometer, as previously described [81]. Xanthine oxidase (0.070 μM final concentration) and hypoxanthine (50 μM final concentration) were used as the superoxide generator in 50 mM phosphate buffer containing 50 μM DTPA at 25 °C.

4.15. Peroxiredoxin 2/cytoglobin competition assay

Aliquots of recombinant human peroxiredoxin 2 and cytoglobin (30 μM each) were reduced with 40-fold excess TCEP on ice for 1 h. TCEP was removed by passing the reduced proteins through freshly prepared 2 ml Zeba Columns. Column preparation included an initial spin at 1000 X G for 2 min to remove storage buffer followed by a wash with 1 ml of ddH_2O. Possible exogenous H_2O_2 was removed by passing 1 ml of 100 mM Phosphate buffer containing 10 μg/ml catalase through each column. The columns were then equilibrated with four −1 ml washes of 100 mM catalase cleared phosphate buffer containing 100 μM DTPA (100 μM Phosphate buffer pH 7.4 was briefly incubated with 10 μg/ml catalase, the buffer was then cleared of catalase by passing it thru a Pall Macrosep advanced 10 000 MWCO filter). 500 μL of each reduced protein was added to the corresponding Zeba columns and spun into fresh tubes. The concentration of peroxiredoxin 2 was determined with a pierce BCA protein kit and the cytoglobin concentration was calculated using the extinction coefficient at the 532 nm peak for $CygbFe^{2+}$. Competition reactions were set up as follows: 2.5 μM peroxiredoxin 2 was mixed with 0, 2.5, 5, 10 and 15 μM recombinant cytoglobin (final concentration), each reaction was treated with 25 μM H_2O_2 for 5 min followed by the addition of 20 mM NEM. 4X non reducing SDS sample buffer was added to each sample and proteins were electrophoresed on 12 % gels until the dye front reached the bottom. The gels were transferred to PVDF membranes and blocked overnight. The primary antibodies were peroxiredoxin 2 (1:15 000), PRX-$SO_{2/3}$ (1:1500), secondary HRP antibodies were either goat anti mouse or goat anti rabbit at 1:2500).

4.16. Statistical analysis

Statistical analyses were performed with GraphPad Prism 9.0. The specific statistical test used to analyze each data set is specified in individual figure legends and p-values are shown in figures. A p-value less than 0.05 was considered statistically significant.

CRediT authorship contribution statement

Frances Jourd'heuil: Writing – review & editing, Writing – original draft, Methodology, Investigation, Formal analysis, Data curation, Conceptualization. **Clinton Mathai:** Writing – original draft, Investigation, Data curation, Conceptualization. **Le Gia Cat Pham:** Investigation. **Kurrim Gilliard:** Investigation. **Joseph Balnis:** Methodology, Investigation. **Katherine A. Overmyer:** Methodology, Investigation. **Joshua J. Coon:** Methodology, Investigation. **Ariel Jaitovich:** Supervision, Methodology, Investigation. **Benoit Boivin:** Writing – original draft, Conceptualization. **David Jourd'heuil:** Writing – review & editing, Writing – original draft, Supervision, Formal analysis, Data curation, Conceptualization.

Declaration of competing interest

The authors declare that they have no known competing financial interests or personal relationships that could have appeared to influence the work reported in this paper.

Acknowledgments

This work was supported by NIH grants RO1 HL142807 (to D.J.), P41 GM108538 (to J.C.C.), RO1 AI173035 and HL160661 (to A.J.), 1R35GM153449 (to B.B.).

Appendix A. Supplementary data

Supplementary data to this article can be found online at https://doi.org/10.1016/j.redox.2025.103633.

Data availability

Data will be made available on request.

References

[1] D. Harrison, K.K. Griendling, U. Landmesser, B. Hornig, H. Drexler, Role of oxidative stress in atherosclerosis, Am. J. Cardiol. 91 (2003) 7A–11A.
[2] J.R. Burgoyne, et al., Cysteine redox sensor in PKGIa enables oxidant-induced activation, Science 317 (2007) 1393–1397.
[3] J.R. Erickson, et al., A dynamic pathway for calcium-independent activation of CaMKII by methionine oxidation, Cell 133 (2008) 462–474.
[4] L.J. Zhu, et al., Oxidative activation of the Ca(2+)/calmodulin-dependent protein kinase II (CaMKII) regulates vascular smooth muscle migration and apoptosis, Vasc. Pharmacol. 60 (2014) 75–83.
[5] H. Knight, et al., Cyclin D-CDK4 disulfide bond attenuates pulmonary vascular cell proliferation, Circ. Res. 133 (2023) 966–988.
[6] X. Tong, X. Hou, D. Jourd'heuil, R.M. Weisbrod, R.A. Cohen, Upregulation of Nox4 by TGFbeta1 oxidizes SERCA and inhibits NO in arterial smooth muscle of the prediabetic Zucker rat, Circ. Res. 107 (2010) 975–983.
[7] I.S. Kil, et al., Feedback control of adrenal steroidogenesis via H2O2-dependent, reversible inactivation of peroxiredoxin III in mitochondria, Mol. Cell 46 (2012) 584–594.
[8] H.A. Woo, et al., Inactivation of peroxiredoxin I by phosphorylation allows localized H(2)O(2) accumulation for cell signaling, Cell 140 (2010) 517–528.
[9] R.F. Queiroz, et al., Hydrogen peroxide signaling via its transformation to a stereospecific alkyl hydroperoxide that escapes reductive inactivation, Nat. Commun. 12 (2021) 6626.
[10] S. Stocker, K. Van Laer, A. Mijuskovic, T.P. Dick, The conundrum of hydrogen peroxide signaling and the emerging role of peroxiredoxins as redox relay hubs, Antioxidants Redox Signal. 28 (2018) 558–573.
[11] C.C. Winterbourn, Hydrogen peroxide reactivity and specificity in thiol-based cell signalling, Biochem. Soc. Trans. 48 (2020) 745–754.
[12] D. Peralta, et al., A proton relay enhances H2O2 sensitivity of GAPDH to facilitate metabolic adaptation, Nat. Chem. Biol. 11 (2015) 156–163.
[13] C. Colussi, et al., H2O2-induced block of glycolysis as an active ADP-ribosylation reaction protecting cells from apoptosis, FASEB J. 14 (2000) 2266–2276.
[14] K.E. Halligan, F.L. Jourd'heuil, D. Jourd'heuil, Cytoglobin is expressed in the vasculature and regulates cell respiration and proliferation via nitric oxide dioxygenation, J. Biol. Chem. 284 (2009) 8539–8547.
[15] F.L. Jourd'heuil, et al., The hemoglobin homolog cytoglobin in smooth muscle inhibits apoptosis and regulates vascular remodeling, Arterioscler. Thromb. Vasc. Biol. 37 (2017) 1944–1955.

[16] C. Mathai, et al., Regulation of DNA damage and transcriptional output in the vasculature through a cytoglobin-HMGB2 axis, Redox Biol. 65 (2023) 102838.
[17] J.L. Zweier, G. Ilangovan, Regulation of nitric oxide metabolism and vascular tone by cytoglobin, Antioxidants Redox Signal. 32 (2020) 1172–1187.
[18] J.L. Zweier, et al., Cytoglobin has potent superoxide dismutase function, Proc. Natl. Acad. Sci. U. S. A. 118 (2021).
[19] P. Beckerson, D. Svistunenko, B. Reeder, Effect of the distal histidine on the peroxidatic activity of monomeric cytoglobin, F1000Res 4 (2015) 87.
[20] T.T. Thuy le, et al., Absence of cytoglobin promotes multiple organ abnormalities in aged mice, Sci. Rep. 6 (2016) 24990.
[21] S. Singh, et al., Cytoglobin modulates myogenic progenitor cell viability and muscle regeneration, Proc. Natl. Acad. Sci. U. S. A. 111 (2014) E129–E138.
[22] E.B. Randi, et al., The antioxidative role of cytoglobin in podocytes: implications for a role in chronic kidney disease, Antioxidants Redox Signal. 32 (2020) 1155–1171.
[23] S. Zhang, et al., Cytoglobin promotes cardiac progenitor cell survival against oxidative stress via the upregulation of the NFkappaB/iNOS signal pathway and nitric oxide production, Sci. Rep. 7 (2017) 10754.
[24] A. Kuehne, et al., Acute activation of oxidative pentose phosphate pathway as first-line response to oxidative stress in human skin cells, Mol. Cell 59 (2015) 359–371.
[25] M. Ralser, et al., Metabolic reconfiguration precedes transcriptional regulation in the antioxidant response, Nat. Biotechnol. 27 (2009) 604–605.
[26] D. Shenton, C.M. Grant, Protein S-thiolation targets glycolysis and protein synthesis in response to oxidative stress in the yeast Saccharomyces cerevisiae, Biochem. J. 374 (2003) 513–519.
[27] R.J. Paul, Smooth muscle energetics, Annu. Rev. Physiol. 51 (1989) 331–349.
[28] M.B. Buechler, et al., Cross-tissue organization of the fibroblast lineage, Nature 593 (2021) 575–579.
[29] E.S. Fry, G.W. Kattawar, R.M. Pope, Integrating cavity absorption meter, Appl. Opt. 31 (1992) 2055–2065.
[30] V.V. Pak, et al., Ultrasensitive genetically encoded indicator for hydrogen peroxide identifies roles for the oxidant in cell migration and mitochondrial function, Cell Metab. 31 (2020) 642–653, e646.
[31] M.N. Hoehne, et al., Spatial and temporal control of mitochondrial H(2) O(2) release in intact human cells, EMBO J. 41 (2022) e109169.
[32] S. Kakar, F.G. Hoffman, J.F. Storz, M. Fabian, M.S. Hargrove, Structure and reactivity of hexacoordinate hemoglobins, Biophys. Chem. 152 (2010) 1–14.
[33] D. Hamdane, et al., The redox state of the cell regulates the ligand binding affinity of human neuroglobin and cytoglobin, J. Biol. Chem. 278 (2003) 51713–51721.
[34] H. Tsujino, et al., Disulfide bonds regulate binding of exogenous ligand to human cytoglobin, J. Inorg. Biochem. 135 (2014) 20–27.
[35] P. Beckerson, M.T. Wilson, D.A. Svistunenko, B.J. Reeder, Cytoglobin ligand binding regulated by changing haem-co-ordination in response to intramolecular disulfide bond formation and lipid interaction, Biochem. J. 465 (2015) 127–137.
[36] P. Beckerson, B.J. Reeder, M.T. Wilson, Coupling of disulfide bond and distal histidine dissociation in human ferrous cytoglobin regulates ligand binding, FEBS Lett. 589 (2015) 507–512.
[37] B.J. Reeder, J. Ukeri, Strong modulation of nitrite reductase activity of cytoglobin by disulfide bond oxidation: implications for nitric oxide homeostasis, Nitric Oxide 72 (2018) 16–23.
[38] A.W. DeMartino, et al., Redox sensor properties of human cytoglobin allosterically regulate heme pocket reactivity, Free Radic. Biol. Med. 162 (2021) 423–434.
[39] A.G. Cox, C.C. Winterbourn, M.B. Hampton, Measuring the redox state of cellular peroxiredoxins by immunoblotting, Methods Enzymol. 474 (2010) 51–66.
[40] P.A. Karplus, A primer on peroxiredoxin biochemistry, Free Radic. Biol. Med. 80 (2015) 183–190.
[41] A.V. Peskin, et al., Hyperoxidation of peroxiredoxins 2 and 3: rate constants for the reactions of the sulfenic acid of the peroxidatic cysteine, J. Biol. Chem. 288 (2013) 14170–14177.
[42] A.C. Haynes, J. Qian, J.A. Reisz, C.M. Furdui, W.T. Lowther, Molecular basis for the resistance of human mitochondrial 2-Cys peroxiredoxin 3 to hyperoxidation, J. Biol. Chem. 288 (2013) 29714–29723.
[43] K.S. Yang, et al., Inactivation of human peroxiredoxin I during catalysis as the result of the oxidation of the catalytic site cysteine to cysteine-sulfinic acid, J. Biol. Chem. 277 (2002) 38029–38036.
[44] H.A. Woo, et al., Reversible oxidation of the active site cysteine of peroxiredoxins to cysteine sulfinic acid. Immunoblot detection with antibodies specific for the hyperoxidized cysteine-containing sequence, J. Biol. Chem. 278 (2003) 47361–47364.
[45] S. Portillo-Ledesma, et al., Differential kinetics of two-cysteine peroxiredoxin disulfide formation reveal a novel model for peroxide sensing, Biochemistry 57 (2018) 3416–3424.
[46] F.M. Low, M.B. Hampton, A.V. Peskin, C.C. Winterbourn, Peroxiredoxin 2 functions as a noncatalytic scavenger of low-level hydrogen peroxide in the erythrocyte, Blood 109 (2007) 2611–2617.
[47] A.V. Peskin, et al., The high reactivity of peroxiredoxin 2 with H(2)O(2) is not reflected in its reaction with other oxidants and thiol reagents, J. Biol. Chem. 282 (2007) 11885–11892.
[48] K.J. Nelson, D. Parsonage, Measurement of peroxiredoxin activity, Curr. Protoc. Toxicol. Chapter 7 (2011). Unit7 10.
[49] S.W. Kang, I.C. Baines, S.G. Rhee, Characterization of a mammalian peroxiredoxin that contains one conserved cysteine, J. Biol. Chem. 273 (1998) 6303–6311.
[50] E.R. Rochon, et al., Cytoglobin regulates NO-dependent cilia motility and organ laterality during development, Nat. Commun. 14 (2023) 8333.
[51] F. Trandafir, et al., Neuroglobin and cytoglobin as potential enzyme or substrate, Gene 398 (2007) 103–113.
[52] D. Li, et al., Cytoglobin up-regulated by hydrogen peroxide plays a protective role in oxidative stress, Neurochem. Res. 32 (2007) 1375–1380.
[53] H. Nishi, et al., Cytoglobin, a novel member of the globin family, protects kidney fibroblasts against oxidative stress under ischemic conditions, Am. J. Pathol. 178 (2011) 128–139.
[54] A. Latina, et al., DeltaNp63 targets cytoglobin to inhibit oxidative stress-induced apoptosis in keratinocytes and lung cancer, Oncogene 35 (2016) 1493–1503.
[55] Y. Okina, et al., TGF-beta1-driven reduction of cytoglobin leads to oxidative DNA damage in stellate cells during non-alcoholic steatohepatitis, J. Hepatol. 73 (2020) 882–895.
[56] N.Q. Dat, et al., Hexa histidine-tagged recombinant human cytoglobin deactivates hepatic stellate cells and inhibits liver fibrosis by scavenging reactive oxygen species, Hepatology 73 (2021) 2527–2545.
[57] U. Oleksiewicz, et al., Cytoglobin has bimodal: tumour suppressor and oncogene functions in lung cancer cell lines, Hum. Mol. Genet. 22 (2013) 3207–3217.
[58] V.N. Hieu, et al., Capacity of extracellular globins to reduce liver fibrosis via scavenging reactive oxygen species and promoting MMP-1 secretion, Redox Biol. 52 (2022) 102286.
[59] N. Kawada, et al., Characterization of a stellate cell activation-associated protein (STAP) with peroxidase activity found in rat hepatic stellate cells, J. Biol. Chem. 276 (2001) 25318–25323.
[60] R.J. Shaw, et al., Cytoglobin is upregulated by tumour hypoxia and silenced by promoter hypermethylation in head and neck cancer, Br. J. Cancer 101 (2009) 139–144.
[61] H. Li, C. Hemann, T.M. Abdelghany, M.A. El-Mahdy, J.L. Zweier, Characterization of the mechanism and magnitude of cytoglobin-mediated nitrite reduction and nitric oxide generation under anaerobic conditions, J. Biol. Chem. 287 (2012) 36623–36633.
[62] A.C. Straub, et al., Endothelial cell expression of haemoglobin alpha regulates nitric oxide signalling, Nature 491 (2012) 473–477.
[63] X. Liu, et al., Cytoglobin regulates blood pressure and vascular tone through nitric oxide metabolism in the vascular wall, Nat. Commun. 8 (2017) 14807.
[64] I. Mimura, et al., Cytoglobin, a novel globin, plays an antifibrotic role in the kidney, Am. J. Physiol. Ren. Physiol. 299 (2010) F1120–F1133.
[65] R. Xu, et al., Cytoglobin overexpression protects against damage-induced fibrosis, Mol. Ther. 13 (2006) 1093–1100.
[66] N. Thi Thanh Hai, et al., Selective overexpression of cytoglobin in stellate cells attenuates thioacetamide-induced liver fibrosis in mice, Sci. Rep. 8 (2018) 17860.
[67] K. Nakatani, et al., Cytoglobin/STAP, its unique localization in splanchnic fibroblast-like cells and function in organ fibrogenesis, Lab. Invest. 84 (2004) 91–101.
[68] D. Anastasiou, et al., Inhibition of pyruvate kinase M2 by reactive oxygen species contributes to cellular antioxidant responses, Science 334 (2011) 1278–1283.
[69] A. Perkins, L.B. Poole, P.A. Karplus, Tuning of peroxiredoxin catalysis for various physiological roles, Biochemistry 53 (2014) 7693–7705.
[70] J. Dalla Rizza, L.M. Randall, J. Santos, G. Ferrer-Sueta, A. Denicola, Differential parameters between cytosolic 2-Cys peroxiredoxins, PRDX1 and PRDX2, Protein Sci. 28 (2019) 191–201.
[71] R. Benfeitas, G. Selvaggio, F. Antunes, P.M. Coelho, A. Salvador, Hydrogen peroxide metabolism and sensing in human erythrocytes: a validated kinetic model and reappraisal of the role of peroxiredoxin II, Free Radic. Biol. Med. 74 (2014) 35–49.
[72] M.C. Sobotta, et al., Exposing cells to H2O2: a quantitative comparison between continuous low-dose and one-time high-dose treatments, Free Radic. Biol. Med. 60 (2013) 325–335.
[73] J.F. Gibson, D.J. Ingram, P. Nicholls, Free radical produced in the reaction of memyoglobin with hydrogen peroxide, Nature 181 (1958) 1398–1399.
[74] P. George, D.H. Irvine, The reaction of metmyoglobin with strong oxidizing agents, Biochem. J. 58 (1954) 188–195.
[75] B.J. Reeder, Redox and peroxidase activities of the hemoglobin superfamily: relevance to health and disease, Antioxidants Redox Signal. 26 (2017) 763–776.
[76] B.J. Reeder, et al., Tyrosine residues as redox cofactors in human hemoglobin: implications for engineering nontoxic blood substitutes, J. Biol. Chem. 283 (2008) 30780–30787.
[77] B.J. Reeder, R.C. Hider, M.T. Wilson, Iron chelators can protect against oxidative stress through ferryl heme reduction, Free Radic. Biol. Med. 44 (2008) 264–273.
[78] J.R. Marcero, R.B. Piel Iii, J.S. Burch, H.A. Dailey, Rapid and sensitive quantitation of heme in hemoglobinized cells, Biotechniques 61 (2016) 83–91.
[79] K.P. Feeley, D.G. Westbrook, A.W. Bray, S.W. Ballinger, An ex-vivo model for evaluating bioenergetics in aortic rings, Redox Biol. 2 (2014) 1003–1007.
[80] K.A. Overmyer, et al., Large-scale multi-omic analysis of COVID-19 severity, Cell Syst. 12 (2021) 23–40, e27.
[81] D. Jourd'heuil, et al., Reaction of superoxide and nitric oxide with peroxynitrite, J. Biol. Chem. 276 (2001) 28799–28805.